Available online at www.sciencedirect.com
SCIENCE DIRECT®
Synthetic Metals 152 (2005) 117–120
SYNTHETIC METALS
www.elsevier.com/locate/synmet

Nano-Crystalline Fullerene Phases in Polymer/Fullerene Bulk-Heterojunction Solar Cells: A Transmission Electron Microscopy Study

H. Hoppe [a,*], M. Drees [a], W. Schwinger [b], F. Schäffler [b], N.S. Sariciftci [a]

[a] *Linz Institute for Organic Solar Cells (LIOS), Physical Chemistry, Johannes Kepler University, Altenbergerstr. 69, A-4040 Linz, Austria*
[b] *Institut für Halbleiter- und Festkörperphysik, Johannes Kepler University, Altenbergerstr. 69, A-4040 Linz, Austria*

Abstract

The nanoscale phase separation in polymer/fullerene bulk heterojunction plastic solar cells requires the use of high resolution techniques for imaging. In this study we used a high-resolution transmission electron microscope (HR-TEM) together with selected area electron diffraction (SAED) to visualize the polymer and fullerene distributions and their amorphous or crystalline organization in the film. While pristine polymer films exhibited no crystalline order, the fullerene organized in nanocrystals. Upon annealing of the blend film, the accompanying phase separation reaches the micron level and fullerene phases aggregate to larger single crystals, as could be seen by SAED.

Keywords: Scanning transmission electron microscopy, electron-solid diffraction, poly(phenylene vinylene) derivative, fullerenes, solar cells

1. Introduction

Plastic solar cells based on conjugated polymer/fullerene blends have been the subject of increasing research interest within the last few years [1-4]. In contrast to the bilayer heterojunction [5], these blends or bulk heterojunctions are characterized by a highly increased interfacial area between the two constituents. Recently it has been found that upon changing the spin casting solvent from toluene to chlorobenzene in MDMO-PPV:PCBM (poly[2-methoxy-5-(3,7-dimethyloctyloxy)]- 1,4-phenylenevinylene):(1-(3-methoxycarbonyl) propyl-1-phenyl[6,6]C_{61}) blends, the power conversion efficiency increased dramatically [6]. This was attributed to a more favourable nanomorphology of the donor and acceptor phases within the film, whereas the finer phase separation yielded the better efficiency. However, different solvents may result in different mobilities within polymer materials [7]. Photoexcitations within organic materials lead in general to Coulombically bound electron-hole pairs (excitons) [8,9]. The excitons may diffuse within the absorbing material until they either decay radiatively or non-radiatively or reach the donor-acceptor interface within their lifetime. If the energy difference between the ionisation potential of the excited donor (I_{D^*}) and the electron affinity of the acceptor (A_A) is larger than the Coulomb binding energy U_C of the exciton, an efficient photoinduced charge transfer occurs at the donor-acceptor interface [10]. Since exciton diffusion lengths in organic materials usually range within 5 to 30 nm [11-17], the donor-acceptor phase separation has to be at the same nanoscale for an efficient charge generation. Once electron and hole are separated onto the acceptor and donor phases respectively, they can either diffuse or drift within the internal electric field towards the contacts. This charge-separated state is rather stable, which is reflected by the large imbalance between forward ($> 10^{13}$ s^{-1}) [18] and backward (10^3-10^6 s^{-1}) [19] transfer rates. Assuming high enough mobilities, the charge carriers will reach the electrodes within their lifetime, and bimolecular recombination can be suppressed. Therefore the dependence of the photocurrent on the incident light intensity can be linear [20,21]. However, for an efficient charge transport percolation of hole and electron transporting phases to the anode and cathode is required. Hence the control of the underlying nanoscale morphology of these organic solar cells is of current research interest [22-26]. These studies have shown that high concentrations of PCBM lead to phase separation within the spin cast blend films. It was concluded, that the films are made up of PCBM aggregates imbedded in a matrix of an equilibrium composition (e.g. saturated solution) of both materials. In this study we use TEM-diffraction, which is capable of distinguishing between amorphous and (multi-) crystalline

* Corresponding author: Tel: +43-732-2468-8854; fax: +43-732-2468-8770; E-mail: harald.hoppe@jku.at

0379-6779/$ – see front matter
doi:10.1016/j.synthmet.2005.07.217

phases, to resolve this question. The results clearly show the crystalline nature of the PCBM clusters and the amorphous nature of the matrix they are embedded in.

2. Experimental

Solutions of MDMO-PPV (Covion, Germany), PCBM (Prof. Hummelen, Universtity of Groningen, The Netherlands) and blends of both were prepared under Argon atmosphere in a glove box system to prevent water contamination. For the pristine PCBM and MDMO-PPV solutions in chlorobenzene, concentrations of 3%wt and 0.25%wt were used respectively. For the blends with ratio 1:4 of MDMO-PPV to PCBM, the polymer concentration was 0.2% in toluene and 0.25% in chlorobenzene solution. Films were spin cast onto glass slides that were covered with a thin layer of sodium metaphosphate (Victawet, SPI Supplies). Afterwards films were floated off the substrate by submerging the glass slide in deionized water and transferred onto Cu TEM grids. After drying films over night in a N_2 flow box, they were studied in a JEOL 2011 FasTEM HR-TEM in bright field mode (at 100 keV).

3. Results and discussion

Thin films were imaged using transmission electron microscopy (TEM), and selected area electron diffraction (SAED) was used to gain information on the local state of crystallinity. The following diffraction images have been inverted, which means that dark regions in the image reflect bright regions on the TEM screen. Also, the central intensity maximum had to be blocked during exposure to protect the CCD camera of the TEM system. This results in a white bar in the inverted diffraction image.

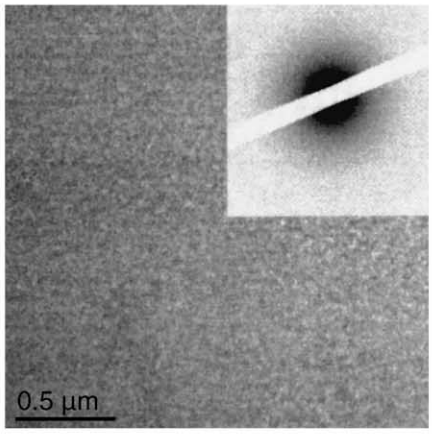

Fig. 1: MDMO-PPV film spin cast from chlorobenzene (0.25%wt) exhibits no order and is completely amorphous.

Figure 1 shows the TEM image of a pristine MDMO-PPV film. It looks homogeneous and there are no different phases that can be distinguished. The grainy background is caused by the noise of the CCD camera. The inset of Figure 1 shows the diffraction pattern of the investigated area. Only the central maximum is observed, there is no sign of fringes (Debye-Scherrer rings) or reflexes caused by crystalline order in the material. From this it can be concluded that (within the resolution of the SEAD) the pristine MDMO-PPV film is amorphous. Pristine PCBM films also don't show any separate phases (compare Fig. 2). In contrast to MDMO-PPV films the diffraction pattern shows regular fringes (inset of Fig. 2). This is a clear sign of a polycrystalline material. Since TEM allows investigating small areas on the order of 100 nm in diameter of the film, it is clear that the PCBM crystals have to be considerably smaller than 100 nm.

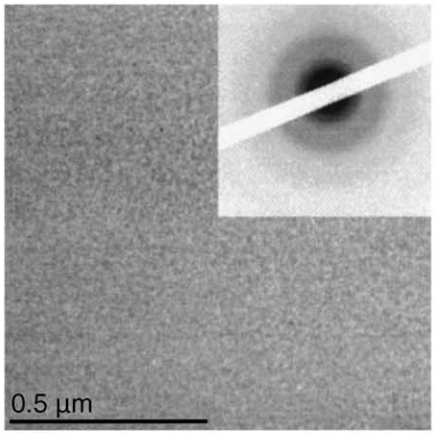

Fig. 2: PCBM films spin cast from chlorobenzene (3%wt) yield some fringes in the electron diffraction pattern, thus indicating a multi-crystalline order in the film on the nanometer scale.

Blending both materials with the weight ratio of 1:4 between MDMO-PPV and PCBM in chlorobenzene and subsequent spin casting yields rather homogeneous films that exhibit some weak features on the sub 100 nm scale.

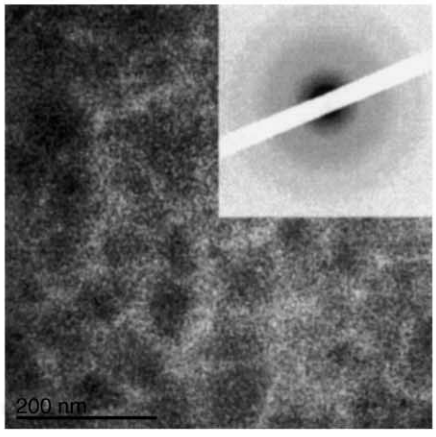

Fig. 3: Blend film of MDMO-PPV:PCBM 1:4 spin cast from chlorobenzene (0.2%wt) yields similar diffraction pattern as found for pristine PCBM films.

Clearly some fringes are visible in the diffraction image, but the underlying order in the film must be smaller than that of the pristine PCBM films, since the fringes are less pronounced. However, there is some local order of the PCBM molecules (compare Fig. 3).

Upon casting the blend with the same composition using toluene as a solvent, a large-scale phase separation is observed. The film exhibits round shaped domains (dark) of up to several hundred nm in diameter (Fig. 4).

This phase has been previously assigned to be PCBM-rich, following the observation of increasing domain sizes for increased PCBM contents in the blends [22,24-26]. The surrounding MDMO-PPV-rich phase was estimated to be a composition of PCBM and MDMO-PPV of roughly the same proportions. Here we find for both the phases fringes in the electron diffraction signal, as depicted in Fig. 4.

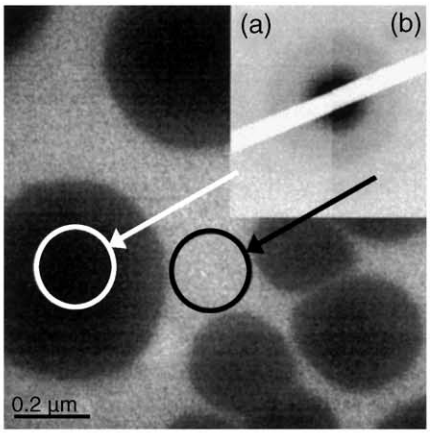

Fig. 4: Blend films MDMO-PPV:PCBM 1:4 spin cast from toluene (0.2%wt) exhibit a larger scale phase separation. Both, the clusters (a) and the area in between (b) the clusters yield fringes in the electron diffraction pattern (inset).

Hence, the MDMO-PPV-rich phase is indeed a composition of MDMO-PPV and PCBM, wherein the PCBM is still organized in a nano-crystalline manner. This phase cannot be bare MDMO-PPV, since bare MDMO-PPV does not exhibit any order in our studies (SAED image in Fig. 1).

On annealing the toluene cast blend film at about 150°C for 4 hours, larger micron sized aggregates are obtained (Fig. 5b), in agreement with earlier results [26]. Single crystalline diffraction images could be obtained on these aggregates (compare Fig. 5c). Now the phase between these crystallites exhibits no sign of any order anymore (Fig. 5d), and it can be concluded that the annealing process results in a true phase separation between MDMO-PPV and PCBM.

Comparison of the diffraction image of the thermally aggregated crystallites with the fringes obtained in the blend films yields good agreement of the radii (Fig. 6). This is a strong indication that the PCBM in the blend is in form of nano-crystallites that form large crystals during the heat treatment.

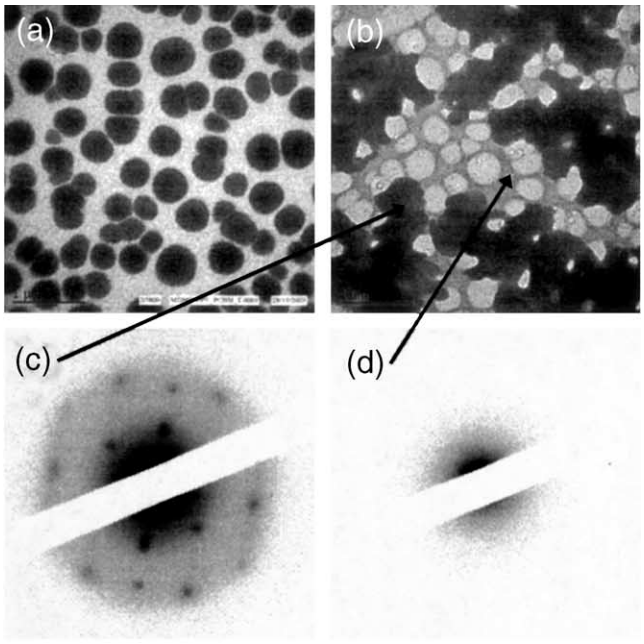

Fig. 5: As cast (a) and annealed (b) blend film of MDMO-PPV:PCBM 1:4 spin cast from toluene (0.2%wt). Large aggregates have formed on the surface of the film during the annealing and thereby the dark PCBM clusters observed in the unheated film were depleted. The large aggregates can produce a single crystalline diffraction image (c), whereas the phase between those crystallites appears to be completely amorphous (d), thus being attributed to the polymer. Therefore the annealing promotes complete phase separation in the film.

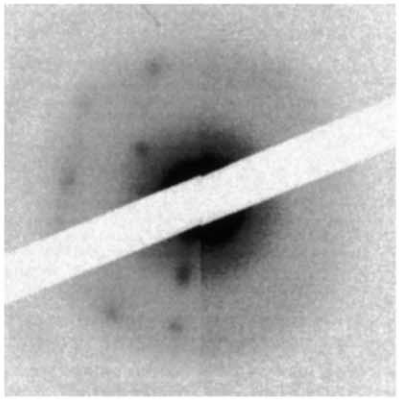

Fig. 6: Comparison of the TEM-diffraction pattern of single crystalline PCBM (left) and multi crystalline PCBM found in the blend films (right).

For C_{60} single-crystals a face centred cubic (fcc) structure was obtained earlier [27]. The unit cell had a lattice constant of a_0=14.2 Å, and the center-to-center distance between the C_{60} molecules with a diameter of 7.1 Å was exactly 10 Å. If we assume an fcc structure for the PCBM crystallites, the fit with the experimental data is satisfactory and we calculate a lattice constant of about 14 Å [27], which is very similar to the C_{60} data of Heiney et al. [28]. This result is intriguing, since PCBM exhibits some side groups, that don't seem to hinder close crystal packing.

It was found that PCBM is capable to organize in crystals when grown from solution [23]. However, due to the crystallization method used, solvent molecules were included in the crystal-matrix. Since the large crystallites in our studies were formed during the annealing process, an inclusion of solvent molecules is very unlikely. Intriguingly the attached side group present on the PCBM does not seem to hinder crystallization or increase the intermolecular spacing as compared to C_{60} crystals. Therefore the ability of close packing will be one of the reasons for the superior charge transport properties of PCBM [29-31]. However, the electron conduction inside the bulk heterojunction solar cell device will be ultimately limited by the transport between adjacent PCBM nano-crystallites and percolated pathways of fullerene domains towards the contact.

Whereas for a blend of C_{60} with poly(3-octylthiophene) the C_{60} organized in rather angular single crystals of up to hundreds of nanometers [32], the PCBM clusters/phases in the blend and pristine PCBM films consisted of much smaller crystallites on the order of nanometers resulting in fringes and not in point pattern in the SAED figures. Thus the PCBM clusters are aggregates of much smaller PCBM nanocrystals. Only upon heat treatment and coarse phase separation we can observe the larger microcrystals. This phase separation is a nano-morphological instability, which can play a crucial role in the long-term stability of these solar cells.

4. Conclusion

In conclusion, TEM in combination with electron diffraction is a powerful tool for the investigation of the nanoscale crystalline phases within solid-state polymer/fullerene blends. The lateral distribution of the phases and phase-separated structures can be followed down to the nanometer scale. It was found that PCBM organizes into multi-crystalline structures on the nanoscale, when cast from solution. However, for annealed blend samples the evolving PCBM microcrystals showed a distinct diffraction pattern. Determination of the crystallographic length scales suggests these phases to be closely packed, similar to the fcc-structure found for C_{60}. An isotropic charge transport with comparably high mobilities in PCBM may be a result of this close packing at the same dimensions as found for C_{60} crystals.

Acknowledgements

Part of this work was performed within the Christian Doppler Society's dedicated laboratory on Plastic Solar Cells co-funded by Konarka Corporation. The TEM images were recorded at the Technical Service Unit (TSE) of the Johannes Kepler University.

References

[1] C.J. Brabec, N.S. Sariciftci, and J.C. Hummelen, Adv. Funct. Mater. 11, 15 (2001).
[2] J. Nelson, Curr. Opin. Solid State Mater. Sci. 6, 87 (2002).
[3] *Organic Photovoltaics: Concepts and Realization*; *Vol. 60*, ed. by C.J. Brabec, V. Dyakonov, J. Parisi, and N.S. Sariciftci (Springer, Berlin, 2003).
[4] H. Hoppe and N.S. Sariciftci, J. Mater. Res. 19, 1924 (2004).
[5] C.W. Tang, Appl. Phys. Lett. 48, 183 (1986).
[6] S.E. Shaheen, C.J. Brabec, N.S. Sariciftci, F. Padinger, T. Fromherz, and J.C. Hummelen, Appl. Phys. Lett. 78, 841 (2001).
[7] W. Geens, S.E. Shaheen, B. Wessling, C.J. Brabec, J. Poortmans, and N.S. Sariciftci, Org. Electron. 3, 105 (2002).
[8] M. Pope and C.E. Swenberg, *Electronic processes in organic crystals and polymers*, 2. ed. (Oxford University Press, New York, 1999).
[9] *Primary Photoexcitations in Conjugated Polymers: Molecular Exciton versus Semiconductor Band Model*; edited by N.S. Sariciftci (World Scientific, Singapore, 1997).
[10] N.S. Sariciftci, L. Smilowitz, A.J. Heeger, and F. Wudl, Science 258, 1474 (1992).
[11] J.J.M. Halls, K. Pichler, R.H. Friend, S.C. Moratti, and A.B. Holmes, Appl. Phys. Lett. 68, 3120 (1996).
[12] J.J.M. Halls and R.H. Friend, Synth. Met. 85, 1307 (1997).
[13] T.J. Savanije, J.M. Warman, and A. Goossens, Chem. Phys. Lett. 287, 148 (1998).
[14] A. Haugeneder, M. Neges, C. Kallinger, W. Spirkl, U. Lemmer, J. Feldmann, U. Scherf, E. Harth, A. Gügel, and K. Müllen, Phys. Rev. B 59, 15346 (1999).
[15] L.A.A. Pettersson, L.S. Roman, and O. Inganäs, J. Appl. Phys. 86, 487 (1999).
[16] M. Stoessel, G. Wittmann, J. Staudigel, F. Steuber, J. Blässing, W. Roth, H. Klausmann, W. Rogler, J. Simmerer, A. Winnacker, M. Inbasekaran, and E.P. Woo, J. Appl. Phys. 87, 4467 (2000).
[17] T. Stübinger and W. Brütting, J. Appl. Phys. 90, 3632 (2001).
[18] G. Zerza, C.J. Brabec, G. Cerullo, S.D. Silvestri, and N.S. Sariciftci, Synth. Met. 119, 637 (2001).
[19] A.F. Nogueira, I. Montari, J. Nelson, J.R. Durrant, C. Winder, N.S. Sariciftci, and C. Brabec, J. Phys. Chem. B 107, 1567 (2003).
[20] P. Schilinsky, C. Waldauf, and C.J. Brabec, Appl. Phys. Lett. 81, 3885 (2002).
[21] T. Yohannes, F. Zhang, M. Svensson, J.C. Hummelen, M.R. Andersson, and O. Inganäs, Thin Solid Films 449, 152 (2004).
[22] T. Martens, J. D'Haen, T. Munters, Z. Beelen, L. Goris, J. Manca, M. D'Olieslaeger, D. Vanderzande, L.D. Schepper, and R. Andriessen, Synth. Met. 138, 243 (2003).
[23] M.T. Rispens, A. Meetsma, R. Rittberger, C.J. Brabec, N.S. Sariciftci, and J.C. Hummelen, Chem. Commun. 17, 2116 (2003).
[24] X. Yang, J.K.J. van Duren, R.A.J. Janssen, M.A.J. Michels, and J. Loos, Macromolecules 37, 2151 (2004).
[25] J.K.J. van Duren, X. Yang, J. Loos, C.W.T. Bulle-Lieuwma, A.B. Sieval, J.C. Hummelen, and R.A.J. Janssen, Adv. Funct. Mater. 14, 425 (2004).
[26] H. Hoppe, M. Niggemann, C. Winder, J. Kraut, R. Hiesgen, A. Hinsch, D. Meissner, and N.S. Sariciftci, Adv. Funct. Mater. 14, 1005, (2004).
[27] The calculation is based on a comparison between the point distances in the observed diffraction pattern with those obtained at the same camera settings for silicon, where the dimensions are known.
[28] P.A. Heiney, J.E. Fischer, A.R. McGhie, W.J. Romanow, A.M. Denenstein, J.P. McCauley Jr., A.B. Smith, and D.E. Cox, Phys. Rev. Lett. 66, 2911 (1991).
[29] V.D. Mihailetchi, J.K.J. van Duren, P.W.M. Bloom, J.C. Hummelen, R.A.J. Janssen, J.M. Kroon, M.T. Rispens, W.J.H. Verhees, and M.M. Wienk, Adv. Funct. Mater. 13, 43 (2003).
[30] C. Waldauf, P. Schilinsky, M. Perisutti, J. Hauch, and C.J. Brabec, Adv. Mater. 15, 2084 (2003).
[31] G.J. Matt, N.S. Sariciftci, and T. Fromherz, Appl. Phys. Lett. 84, 1570 (2004).
[32] N. Camaioni, M. Catellani, S. Luzzati, and A. Migliori, Thin Solid Films 403-404, 489 (2002).